Image Texture Descriptors to Quantify Bilateral Filter on Low Dose Computerized Tomography

A. R. AL-Hinnawi and M. Daear

Medical Imaging & Image processing Research Group,
Biomedical Engineering Dept., Damascus University, Syria
arhmb@scs-net.org

Abstract

Reducing the Radiation Dose in Multi Slice Computerized Tomography MSCT/CT is a significant concern. The Non-Linear Bilateral Filter BF was proved to have the property of de-noising digital images without jeopardizing the fine structures. This paper tests the BF performance on low dose CT by using Image Texture Metrics which have not been reported in literature. Set of CT images of dedicated CT phantom were acquired at four different radiation doses by means of minimizing the X-Ray Tube Current. As radiation dose is lowered, the noise will unavoidably increase degrading the diagnostic value of the CT image. The BF was applied to achieve image space noise removal. The value of each BF parameter was changed set of times. The quantitative assessment of the amount of noise reduction was done using eight metrics based on image texture descriptors that have not been tried before. Particularly, we used three histogram moments (Variance, Skewness, Kurtosis) and five co-occurrence matrix descriptors (Correlation, Contrast, Uniformity, Homogeneity, Entropy). The results showed that these descriptors are reliable metrics to assess BF performance. Each image descriptor value -after applying BF on low dose CT images- is enhanced toward the full dose CT image. Therefore, these metrics have provided additional proofs about the capability of BF toward enhancing the diagnostic value of the low dose MSCT. We concluded that: 1-) Texture descriptors are reliable measures similar to other metrics that are commonly used in literature, and 2-) BF can contribute to reduce X-Ray dose in routine CT. Also, the results have leaded to propose the effective procedure to employ BF on CT.

Keywords: *Bilateral Filter; Image Texture Descriptors; Histogram Moments; Co-occurrence Matrix Descriptors; MSCT/CT Radiation Dose Reduction*

1. Introduction

Multi-slice computerized tomography MSCT/CT exposes patients with the highest radiation dose among other X-Ray diagnostic imaging devices [1, 4]. Hence, any attempt to reduce radiation dose is of great essence. However, as radiation dose decreases the image quality is degraded because of the increase of the image noise [1-3].

MSCT researchers have introduced set of approaches to reduce radiation does [1, 4]. One of which is the applied techniques on the CT image domain. This include software digital image processing filtering solutions for noise reduction either at Image space (i.e. reconstructed image) or projection space (i.e. sinogram).

Many image processing filters were introduced in literature. Chun-yu et al explored the Median and adaptive Median filters [5]. They used the peak signal noise ratio PSNR and the deterioration degree to evaluate filters performance on CT Chest image with various added noise density (i.e. salt and paper noise). Kelm et al evaluated the non-local mean NLM filter [6]. They also used PSNR to test the filter's function on CT Chest phantom. Lanzolla et. al., tested the Gaussian, Averaging, and Un-sharp smoothing filters followed with applying Perwitt and Sobel edge preserving filters [7]. They measured the PSNR on CT chest image with added zero mean guassian noise. Attivissimo et al continued the previous work and apply Anisotropic Diffusion filter [8]. They used the relative mean square error MSE to evaluate filter performance. On the other hand, there are published researches in the projection space domain for de-noising CT images. One of which is the experiment done by Li et. al., [9]. They generated analytical relationship between variance and mean of probability distributed function PDF in order to guide 2-D sinogram smoothing process.

Bilateral Filter BF is a nonlinear filter developed in 1998 by Tomasi and Manduchi [10]. By careful selection of BF parameters, BF has the ability to smooth any arbitrary digital image while preserving the edges (i.e. fine information). This property was repeatedly deduced by researches such as Vijaya and Feng et. al., [11, 12]. They used PSNR, Donoho's method, or wavelet based method in order to estimate the noise variations on non-medical digital images.

The BF functioning on CT images was tested to find out its efficacy in CT dose reduction. Giraldo et al demonstrated that dose reduction up to 20 folds can be obtained from Gradient Adaptive BF as applied on animal perfusion CT [13]. They measured the time attenuation curves on CT images acquired at different folds of exposures. They inferred that the 20 fold dose reduction keep the image quality comparable with the full dose image. Also, Giraldo with other colleagues compared the performance of BF and NLM filters on CT images [14]. They tested the filters on both phantom and abdomen CT images acquired from dual source CT system. The assessment was done using spatial resolution module, local contrast module, line profile, and the radiologist opinion. They deduced that both filters de-noise the CT image quite well, but NLM needs careful choose of its parameters. Steckmann and Kachelrieβ found that BF can be used to reduce the blooming artifact encountered during applying reconstruction kernels in Cardiac CT [15]. Huang et al employed Ancombe transform and Block Matching with 3-D filtering BM3D to reconstruct CT images of Shepp-logan phantom [16] (sinogram space). Then, they applied NLM or BF filters on the CT images to preserve edge information (image space). They calculated SNR and normalized mean square error NMSE for evaluation. Finally, Manduca et al adopted an algorithm based on BF filtering applied on CT image space [17]. The BF was applied on thin wire phantom, contrast plate phantom, CT colonography data, and five abdominal low-energy (80 kV) CT exams. They found that BF is qualified to improve the SNR without jeopardizing image quality. Consequently, they proposed that BF can lead to considerable dose reduction.

This paper focus on applying BF on CT image space. We noted that the image texture descriptors have not been used to assess BF performance. In this paper, we observed the BF performance on four low dose images of CT plastic phantom by measuring eight image texture metrics based on histogram moments and co-occurrence matrix.

2. Theory

2.1. Bilateral Filter

Bilateral filter is a non-linear digital filter introduced in 1998 [10]. This filter is recommended for images -such as CT- so that removing noise is achieved without harshly loosing edge information. The BF coefficient weights are determined according to both the variation in pixels intensities and the location of pixels in a certain neighborhood. Hence, each pixel will have different BF coefficients based on their geometric closeness and their intensity similarity with the pixel in the center of the BF window NxN. The BF is equated as:

$$I_{BF}(x,y) = \frac{1}{K} \sum_{x,y=(\hat{x},\hat{y})-N}^{(\hat{x},\hat{y})+N} e^{-\frac{\|x-\hat{x}\|^2+\|y-\hat{y}\|^2}{2{\sigma_d}^2}} e^{\frac{-(I(x,y)-I(\hat{x},\hat{y}))^2}{2{\sigma_r}^2}} I(\hat{x},\hat{y}) \quad \dots \quad (1)$$

Which {K} is a normalization constant given by :

$$K = \sum_{x,y=(\hat{x},\hat{y})-N}^{(\hat{x},\hat{y})+N} e^{-\frac{\|x-\hat{x}\|^2+\|y-\hat{y}\|^2}{2{\sigma_d}^2}} e^{\frac{-(I(x,y)-I(\hat{x},\hat{y}))^2}{2{\sigma_r}^2}} \quad \dots \quad (1.1)$$

Equation (1.2) shows that the BF Filter Range is determined by an input constant denoted as [σ_r], whereas Equation (1.3) states that the BF Filter Domain is determined by another input constant called as [σ_d].

$$e^{\frac{-(I(x,y)-I(\hat{x},\hat{y}))^2}{2{\sigma_r}^2}} \dots (1.2) \quad , \quad e^{-\frac{\|x-\hat{x}\|^2+\|y-\hat{y}\|^2}{2{\sigma_d}^2}} \quad \dots \quad (1.3)$$

Hence, the BF has three main parameters. These are the BF window size, the BF filter range, and the BF filter domain.

2.2. Digital Image Texture Descriptors

Image Texture descriptors are a common image processing tools that can be used to evaluate the image coarseness and regulatory [18]. Histogram Moments and Co-occurrence matrix descriptors are two types of statistical methods to describe Image Texture.

2.2.1. Histogram Moment: These are directly applied on the gray level of the pixels in the image. The moment {μ} of order *n* of gray levels in an image is given by:

$$\mu_n(z) = \sum_{i=1}^{L}(z_i - m)^n p(z_i) \dots (2) \quad where \quad m = \sum_{i=1}^{L} z_i p(z_i) \dots (2.1)$$

where: {*l*} is the number of discrete intensities in an image; {*z*} is a variable used for pixel intensity (i.e. gray level); {n} is the Moment order; {*p*[z_i]} is the probability of the pixel intensity z_i; {m} is the mean of pixel intensities in the image; {$\mu_n(z)$]} is the moment {*n*} with respect to the mean.

Gonzales and Woods [18] explained that the second order moment (i.e. n=2) indicates the *Variance* in pixel intensities; The third order (i.e. n=3) is denoted as "*Skewness*" which indicates the sharpness of the histogram slope; Finally, the fourth order (i.e. n=4) is used to describe the flatness of the image histogram and called as "*Kurtosis*". The moment of higher orders do not directly correspond to the shape of histogram so they do not present useful differentiators [18].

2.2.2. Co-occurrence Matrix Descriptors: Histogram moments evaluate the distribution intensities of pixels in an image, but it does not consider the relative position of pixels with respect to each other (i.e. spatial distribution). Co-occurrence matrix CM examines both the distribution of intensities and relative positions of pixels in an image [18].

The CM calculates how many times each pair of intensities happen in an image. The repeated occurrence is also restricted to the preset neighborhood connectivity conditions.

There are set of Image descriptors which can be derived from the CM in which they describe the overall texture of image. We used five CM descriptors: Uniformity, Entropy, Correlation, Homogeneity, and Contrast. Their equations are listed below.

$$\text{Uniformity} = \sum_{i=1}^{K}\sum_{j=1}^{K} P_{ij}^2 \quad \dots(3), \qquad \text{Entropy} = -\sum_{i=1}^{K}\sum_{j=1}^{K} P_{ij}\log_2 P_{ij} \quad \dots \quad (4)$$

$$Correlation = \sum_{i=1}^{K}\sum_{j=1}^{K} \frac{(i-m_r)(j-m_c)P_{ij}}{\sigma_a \sigma_b} \quad \text{where } \sigma_a \neq 0, \sigma_b \neq 0, \quad \dots(5)$$

$$\text{Homogenity} = \sum_{i=1}^{K}\sum_{j=1}^{k} \frac{P_{ij}}{1+|i-j|} \quad \dots(6) \qquad \text{Contrast} = -\sum_{i=1}^{K}\sum_{j=1}^{K} (i-j)^2 P_{ij} \quad \dots \quad (7)$$

Where: {k x k} is the size of the CM; {i, j} are the discrete gray levels; {Pij} is the probability for discrete value {i} to occur beside the discreet value {j}; $\{m_r\}$ and $\{m_c\}$ are the mean of gray levels in row and column, respectively; $\{\sigma_a\}$ and $\{\sigma_b\}$ are the standard deviation of gray levels in row and column, respectively.

Gonzales and Woods [18] explained that Equation (3) calculates the Uniformity (also called Energy) of the image. Whereas, equation (4) measures the randomness of the elements in the CM and it is called Entropy. Equation (5) quantifies how Correlated is a pixel to its neighbor over the entire image. Finally, Equation (6) computes the spatial closeness of the distribution of elements in CM to the diagonal, it is named as Homogeneity; Whereas, Equation (7) measures the Contrast between pixel and its neighbor in the CM image.

3. Materials

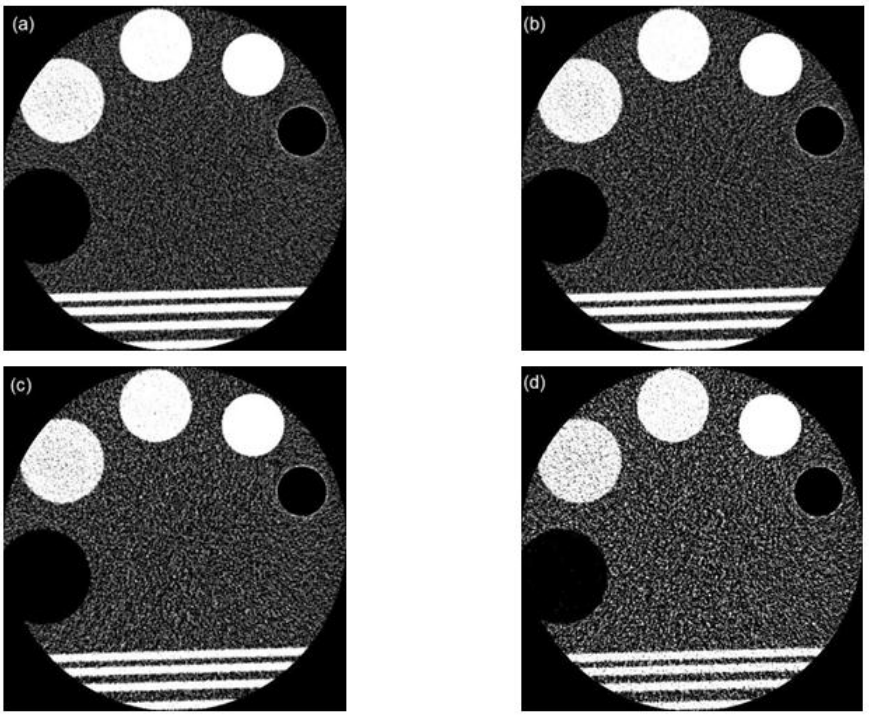

Figure 1(a-d). CT Phantom Images at four different dose exposures. (a) 200mA, (b) 150mA, (c) 100mA, and (d) 50mA

Four images of TOSHIBA CT Phantom were acquired at four different tube currents from a 4 slices TOSHIBA Helical CT model "Aquilion". The selected tube currents are: 200, 150. 100, and 50mA while the tube potential was held at 120 KV. If we choose the 200mA image as a reference, the other images would be 75%, 50% and 25% decrement in radiation dose. The 200mA was selected as a reference because it is a frequently routine clinical procedure. Figure 1 shows those acquired images. The slice thickness was selected to be 2 mm which is believed to be adequate to do the research.

Figure 2 illustrates the variations in image texture due to X-Ray dose variations. A line profile of the pixels intensities at the background of the phantom was calculated. We selected a line profile of 45 pixels for the sake of demonstration. The position of this line profile is illustrated in Figure 2(a) as a red line whereas the red square is going to be used later in the discussion. Figure 2(b) shows the resulting line profiles. The red, green, yellow and blue lines indicate the pixels intensities line profile for 200, 150, 100, and 50 mA dose, respectively. The figure illustrates that as radiation dose is reduced the pixel intensity fluctuations increases. Therefore, CT image texture varies with radiation dose.

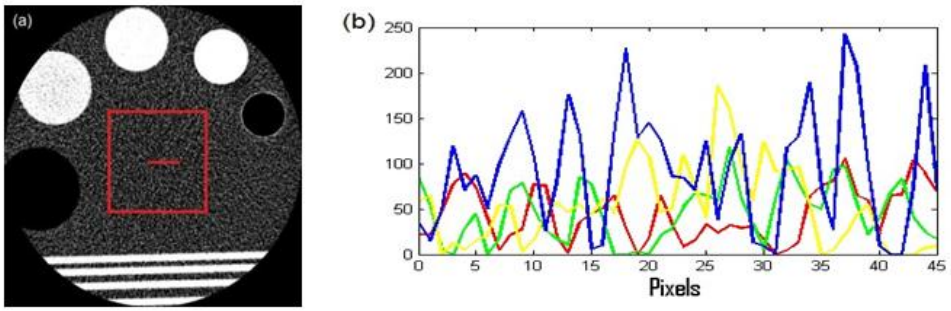

Figure 2. (a) The Location of Line Profile and ROI (i.e. Red line and square). (b) Line Profiles of Pixel Intensities for all Low Dose images (Red:200mA, Green:150mA, Yellow:100mA, and Blue:50mA)

4. Method

The BF was applied on the CT images employing different values of [σ_d] and [σ_r]. The values of [σ_d] were altered in the following steps: 0.5, 1, 2, 3, 4, 5, 6, 7, and 10. Whilst, the values of [σ_r] were changed in the following steps: 0.05, 0.1, 0.2, 0.3, 0.5, and 1. The trial was to keep a fixed value for [σ_r], then apply BF according to the above-mentioned different values for [σ_d]. The window size of the BF was set to be 7x7.

This experiment was done on the 150, 100, 50mA images. Each time after applying the BF at certain value of [σ_r] and [σ_d], histogram moments in equation (2) were calculated with n=2-4. Also, the co-occurrence matrix CM was generated; then the five descriptors in equations (3-7) were calculated. We chose the 8-nieborhood adjacency condition for the CM generation since it is the general case [18].

The BF was not applied on the 200mA image but the histogram moments and the CM descriptors were measured. The resulting values are used as references to see how much close the BF can bring the low dose images to the 200mA image.

5. Results

Figures 3-10 showed the resulting descriptors values from changing [σ_d] at different [σ_r] values. Each figure shows three curves representing one image descriptor calculated after applying BF to the three different dose images. Each figure also contains a straight line which represents the descriptor's value from the 200mA image plotted as a reference.

5.1. Co-occurrence Matrix Descriptors

5.1.1. CM Image Uniformity/Energy: The values of this descriptor should be in the range "0" to "1" according to equation (3) [18]. When Uniformity is "1", this means that the image is a constant gray level image and CM has only single value. Since the low dose image contains higher percentage of noise, it should exhibit low uniformity in comparison to the high dose image. As noise is removed by BF, the uniformity should enhance. Figures 3(a-b) confirm this fact. They show that the 200mA image have the highest energy before applying BF. The uniformity of all low dose images has improved after applying BF for any σ_r and σ_d values. The best values is when $0<\sigma_d\leq 3$ and $0.05\leq\sigma_r<1$. Beyond these limits ($\sigma_d>3$), the curves start to reach constant state and become closer to "1" indicating high level of noise reduction by BF. If $\sigma_r=1$ was selected the working zone becomes linear only within the range $0<\sigma_d\leq 1$. These figures show that Uniformity can observe noise removal by BF.

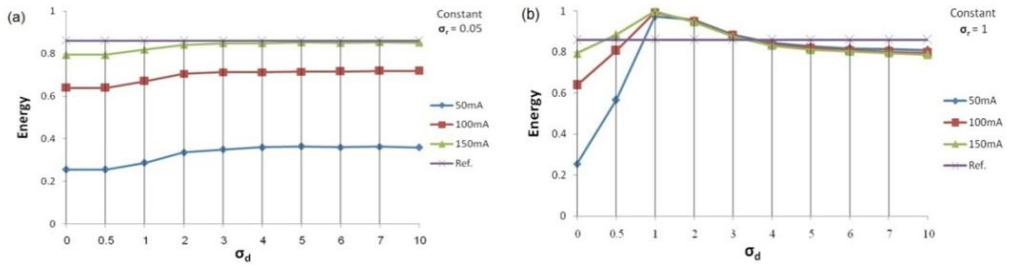

Figure 3. Uniformity/Energy Results for the BF Low Dose Images at Various σ_d Values at: (a) σ_r=0.05 (left) and (b) σ_r=1 (right)

5.1.2. CM Image Entropy: Equation (4) states that the maximum expected value is $2 \log_2 K$. The maximum value happens when all P_{ij} have similar values, corresponding to equal repetition of gray levels co-occurrences [18]. This mimics the case of high noise pattern. Therefore, as dose decreases the entropy should increase because of the increase of noise pattern in the image. This fact is supported in Figure 4(a-b) in which all the low dose images present higher Entropy value than the 200mA image before applying BF. After applying the BF, entropy starts to decrease because of noise removal. For all low dose images, the curves in the figures showed that the useful operating part of the curves take place when $0<\sigma_d\leq4$ and $0.05\leq\sigma_r\leq1$. Beyond this limit, there is no significant variation in Entropy. These figures also illustrate that Entropy is a successful metric to monitor the noise removal by BF.

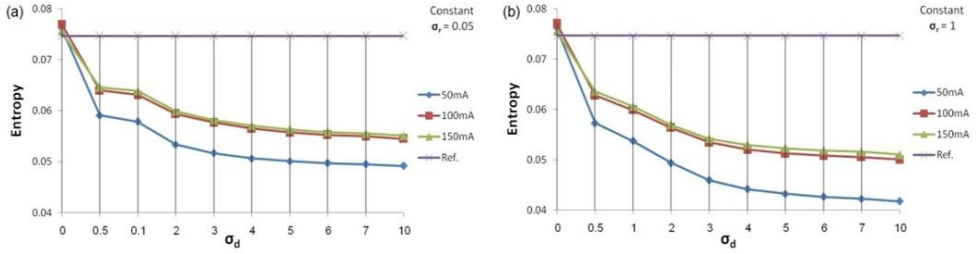

Figure 4. Entropy Results for the BF Low Dose Images at Different σ_d Values at: (a) σ_r=0.05 (left) and (b) σ_r=1 (right)

5.1.3. CM Image Correlation. Equation (5) states that the correlation varies between -1 to +1, corresponding to perfect negative and perfect positive correlation between pixels [18]. Therefore, one anticipates that low dose images should possess low correlation in comparison to the high dose image. This is due to the fact that the low dose image exhibits lower quality than the high dose one. Figures 5(a-b) show that all low dose images displayed lower correlation than the 200mA image. The BF improves the correlation between pixels due to noise removal. The working zone is when $0<\sigma_d\leq3$ and $0.05\leq\sigma_r\leq1$. Beyond these limits, the curves reach steady state indicating no significant variation in the correlation value. These figures disclosed that the correlation can be used as a quantifier to the noise removal by BF.

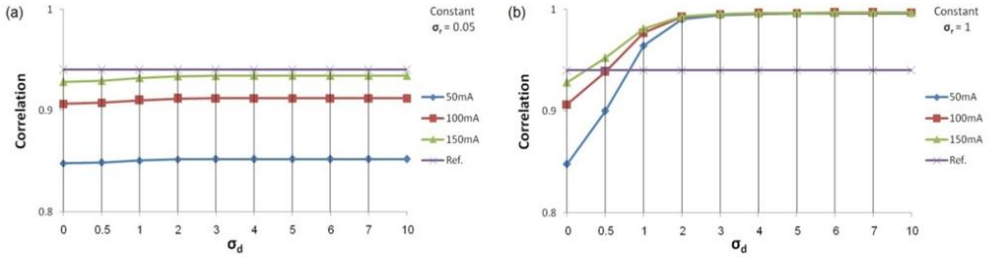

Figure 5. Correlation Results for the BF Low Dose Images at Different σ_d Values at: (a) σ_r=0.05 (left) and (b) σ_r=1 (right)

5.1.4. CM Image Homogeneity: The value of this descriptor is in the range "0" to "1" as equation (6) states [18]. When homogeneity is "1", this means that all gray levels in the image have equal repetition. Therefore, as noise is increased in the image the homogeneity should decrease. In other words, the high dose image has higher homogeneity than the low dose image. This is proved in Figures 6(a-b). They show that the 200mA image has higher homogeneity than all low dose images before applying BF. The BF improves the homogeneity when $0.05 \leq \sigma_r \leq 1$ and $0.5 < \sigma_d \leq 4$. Beyond the previous limits, homogeneity increases till it reaches steady values indicating, again, the excessive smoothing of the images. However, it is true to conclude that homogeneity is also a possible quantifier to the amount of noise removal by BF. Also, if $\sigma_d < 0.5$ and $\sigma_r = 1$ there is a slight decrease in homogeneity. This means that we should always select $\sigma_d > 0.5$ with this metric.

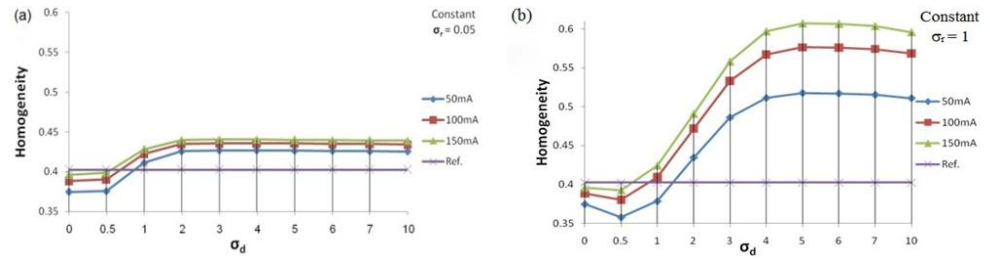

Figure 6. Homogeneity Results for the BF Low Dose Images at Different σ_d Values at: (a) σ_r=0.05 (left) and (b) σ_r=1 (right)

5.1.5. CM Image Contrast: according to Equation (7), CM contrast varies between 0 to $[k-1]^2$. When its value is "0", this means that the CM is constant; hence, noisy images lead to high CM contrast [18]. Hence, one expects that the low dose images should have higher CM contrast than the 200mA image because they contain higher percentage of noise. This is confirmed in Figures 7(a-b). Applying BF has improved all low dose images. The figures showed that the useful zone is when $0 < \sigma_d \leq 3$ and $0.05 \leq \sigma_r \leq 1$. Curves reach steady values when the BF is applied at higher σ_r and σ_d values than the previous limits. Hence, Contrast of the CM can also be used to successfully observe the noise removal by BF.

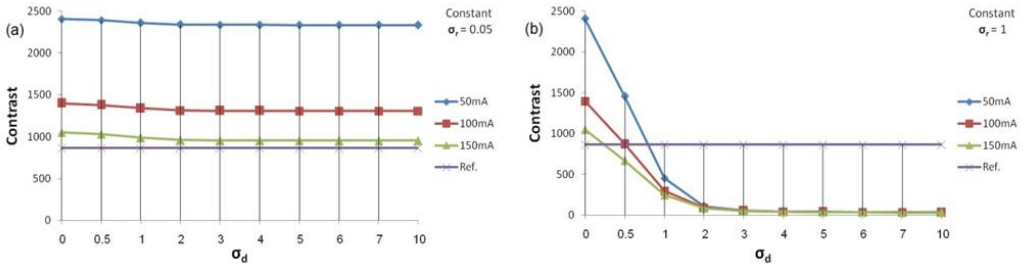

Figure 7. Contrast Results for the BF Low Dose Images at Different σ_d Values at: (a) σ_r=0.05 (left) and (b) σ_r=1 (right)

5.2. Histogram Moments

5.2.1. Variance: It is the second moment which tells us about the histogram uniformity. Histogram variance increases as dose decreases due to noise increase. Therefore, one expects that the low dose images show higher variance than the high dose images. This is confirmed in Figures 8(a-b). They reveal that the lower the dose the higher the variance before applying BF. The variance of all low dose images improve after applying BF for any σ_r and σ_d values. The figures show that the optimum working zone for all low dose images is when $0<\sigma_d\leq4$ and $0.05\leq\sigma_r\leq1$. Again, curves reach steady values when the BF is applied at higher σ_r and σ_d values than the previous limits. However, Variance can effectively quantify the amount of noise removal of BF.

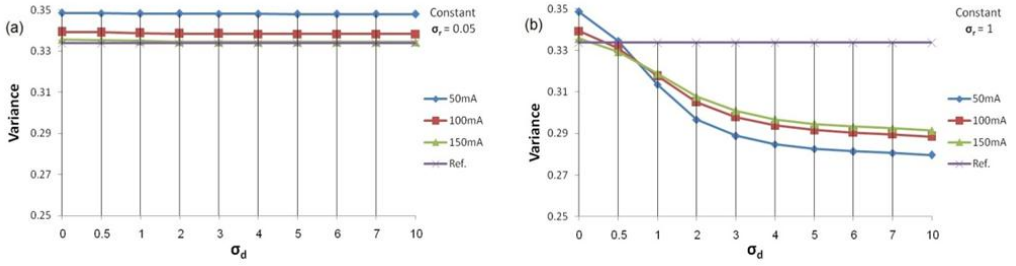

Figure 8. Variance Results for the BF Low Dose Images at Different σ_d Values at: (a) σ_r=0.05 (left) and (b) σ_r=1 (right)

5.2.2. Skewness: It is the third histogram moment which measures the sharpness of the image histogram. As the dose increases the amount of noise decreases leading to sharp histogram slopes because the better image quality of the objects in the image. This, in turn, gives higher skewness value. Figures 9(a-b) have proved this fact because they show that the lower the dose the lower the skewness is. Applying BF enhances the skewness. The curves in the figures show that the ideal part for all low dose images is when $0<\sigma_d\leq3$ and $0.05\leq\sigma_r\leq1$. These figures imply that skewness is a possible effective quantifier of noise removal by BF.

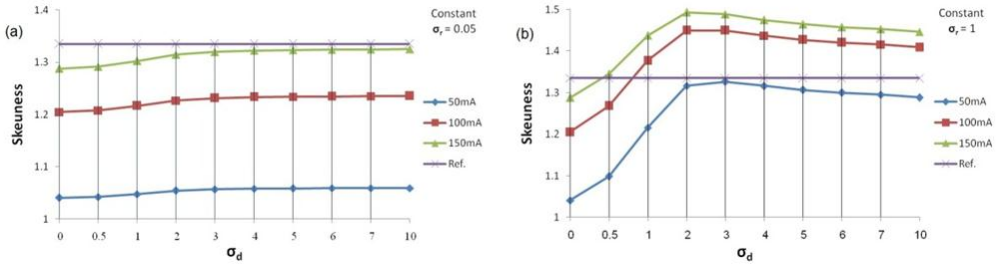

Figure 9. Skewness Results for the BF Low Dose Images at Different σ_d Values at: (a) σ_r=0.05 (left) and (b) σ_r=1 (right)

5.2.3. Kurtosis. This is the fourth histogram moment that estimates the flatness of the image histogram. In low dose image the noise increases affecting the spatial resolution of an image. This should lead to decrease the histogram flatness (i.e. Kurtosis). Figures 10(a-b) have verified this fact because they show that all low dose image exhibit low kurtosis. Applying BF decreases the amount of noise and consequently increases the kurtosis. The figures show that the optimum working zone for all low dose images is when $0<\sigma_d<3$ and $0.05\leq\sigma_r\leq1$; whilst, curves reach steady values when the BF is applied at higher σ_r and σ_d values.

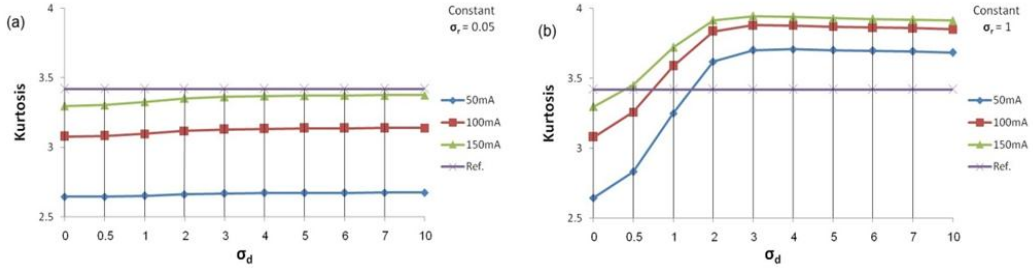

Figure 10. Kurtosis Results for the BF Low Dose Images at Different σ_d Values at: (a) σ_r=0.05 (left) and (b) σ_r=1 (right)

6. Discussion

Figures 3-10 have revealed that all descriptors can be used to measure the noise removal after applying BF similarly to other common metrics, which are used to observe the BF performance, such as the SNR [5-7, 11-12, 16-17] or the MSE [8,16]. The entropy curves in Figure 4(a-b) showed that it has the highest slope for $\sigma_d<0.5$. This means it exhibits the highest sensitivity to any small variance in σ_r and σ_d. Whilst, figure 6(b) show that σ_d should be at least bigger than 0.5 in order to use homogeneity as a metric (i.e. $\sigma_d\geq0.5$).

Table 1 summarizes the optimum BF values for σ_r and σ_d which allow each texture descriptor to quantify the BF performance. This table discloses that the general BF optimum parameters for all Texture descriptors is choosing $0.05\leq\sigma_r\leq1$ and $0<\sigma_d\leq3$. These limits guarantee that all texture descriptors will successfully quantify the noise removal by BF. Choosing $\sigma_r<0.05$ should not affect the previous finding.

However, it is important to mention that these results are obtained for this CT phantom. Although choosing other phantom or clinical MSCT image may need different optimum σ_r

and σ_d zones than those listed in Table 1, it is still valid to claim that these texture descriptors have the potential to quantify the noise removal by BF on low dose CT images.

Table 1. BF Optimum Parameters for each Texture Descriptor to Observe the BF Noise Reduction on Low Dose MSCT Images

		σ_r	σ_d
Co-occurrence Matrix Descriptors	Uniformity/Energy	$0.05 \le \sigma_r < 1$	$0 < \sigma_d \le 3$
	Entropy	$0.05 \le \sigma_r \le 1$	$0 < \sigma_d \le 4$
	Correlation	$0.05 \le \sigma_r \le 1$	$0 < \sigma_d \le 3$
	Homogeneity	$0.05 \le \sigma_r \le 1$	$0.5 < \sigma_d \le 4$
	Contrast	$0.05 \le \sigma_r \le 1$	$0 < \sigma_d \le 3$
Histogram Moment	Variance	$0.05 \le \sigma_r \le 1$	$0 < \sigma_d \le 4$
	Skewness	$0.05 \le \sigma_r \le 1$	$0 < \sigma_d \le 3$
	Kurtosis	$0.05 \le \sigma_r \le 1$	$0 < \sigma_d \le 3$

Also, there is a second point that it needs to be clarified. Despite the fact that the curves in Figures 3-10 are in some cases have intersected its measured value on the full dose image, this does not imply that the image quality of the BF low dose image becomes similar to the quality of the full dose image. Occasionally, the curves come to value better than that obtained from the full dose image. This also does not imply that the BF low dose image exceeds the quality of the full dose image. To further explain this point we generated the Histogram Accumulation at region of interest ROI of the full dose image and the low dose image after and before applying BF. This was done selecting σ_r and σ_d values within the ranges listed in Table 1. The ROI is shown as red square in Figure 2(a). Figures 11(a-c) show the results. These figures demonstrate that applying BF on low dose images enhance the low dose image toward the appearance of full dose image. This conclusion is more obvious on the 100 and 50mA than the 150mA. On the other hand, careful selection of BF parameters for the 150mA image may come very close to the appearance of the 200mA image. This confirms that BF can contribute to reduce X-Ray dose in routine MSCT.

The previous argument (i.e. BF low dose image never reaches the same appearance of the full dose image) can be attributed to the fact that BF removes noise without affecting edges of the image is not an absolute statement. Actually the correct is to say that as BF parameters are low the BF effect on edges is very minimal to be observed. When BF parameters (σ_r and σ_d) start to increase the BF effect on edges starts to increase as well.

Hence, as far as the CT is concerned, the BF has a successful role in enhancing the low dose images by removing the resulting noise in the low dose CT images as long as low values for σ_r and σ_d are selected. This shall expand the diagnostic value of the low dose CT image. However, it will not reach the same quality of the full dose image or any higher dose image. What has been lost due to lowering the dose cannot be retrieved.

Therefore, we propose that the ideal scenario using BF is to be applied as a real-time procedure on the CT image until the radiologist satisfaction. Simple algorithm can be added to the current CT systems. The algorithm should have two key bars allowing the radiologist to select a value for [σ_r] and adjust the values of [σ_d] or vice versa. From the experiments, we suggest that the best way is to set a small value to [σ_r] and change values of [σ_d] until the satisfaction of observer. The size of the BF window can be added as another option. We expect that this scenario will help in expanding the diagnostic value of the low dose CT

images. For instance, it may allow medical physicist to examine pediatrics or to enroll serial CT imaging of young patients. Finally, this strategy will adapt elegantly with the fact that radiologist visual perception to the radiographic CT features varies among them (i.e. using the same preset value of $[\sigma_r]$ and $[\sigma_d]$ for all CT images will not take in consideration the variation in the radiologist perception and experience).

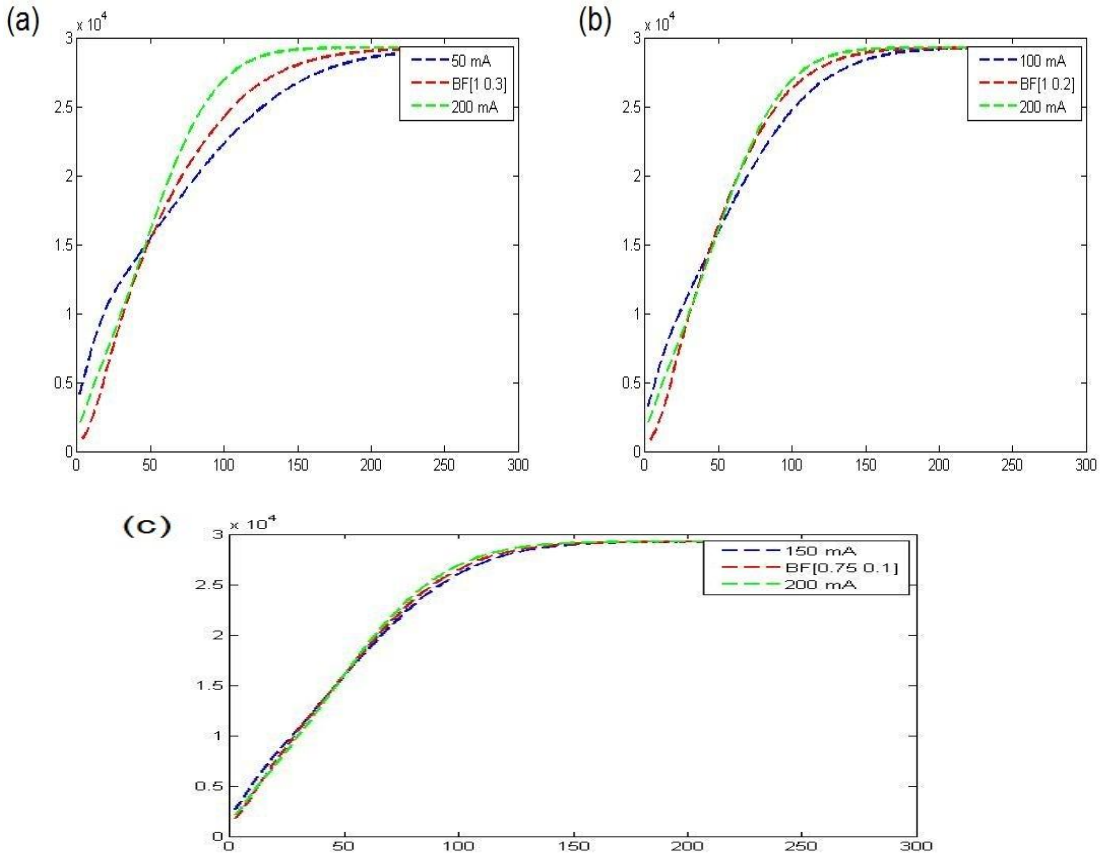

Figure 11. ROI Histogram Accumulation for: (a) 200mA and 50mA image before and after apllying BF with σ_r=0.3 and σ_d=1, and (b) 200mA and 100mA image before and after apllying BF with σ_r=0.2 and σ_d=1, and (c) 200mA and 150mA image before and after apllying BF with σ_r=0.1 and σ_d=0.75

In comparison to literature, this paper tested new metrics (Figures 3-10) to evaluate the BF performance on low dose CT phantom images. All these metrics have showed that they are possible quantifier to noise removal from low dose images by BF. However, we expect the CM descriptors would be more precise than histogram moments because they take in consideration the recurrence of grey levels unlike the histogram moments which are global measures. Also, as the experiments were focusing on the previous findings, this paper also supported the work in literature that BF has the potential to contribute to reduce X-Ray dose in routine CT.

The validation of these results on clinical CT exams, which are believed to be more complex than the phantom, can be forwarded to future research. We expect that the findings of this paper will not be affected.

7. Conclusions

We tested the feasibility of using Image Texture descriptors to evaluate the BF performance on noise reduction of low dose CT images. The phantom images were collected from a CT device at four different radiation doses by means of changing tube current. After applying BF with various combination of σ_r and σ_d values, the amount of noise removal was assessed by calculating three histogram moments and five CM descriptors. All these descriptors showed capability in quantifying the BF performance on low dose CT images.

Also, the results in this paper support the potential of BF in removing noise from low dose CT images. So, the diagnostic value of low dose CT is subject to be enhanced. However, the results showed that this is restricted by selecting low values of σ_r and σ_d.

Additionally, observing the role of filter range σ_r and filter domain σ_d has led us to state that the best scenario to use BF is to set a small value of [σ_r] and modify [σ_d] until the satisfaction of observer. Inverting the BF parameters scenario is also possible. This maintains the finding in literature that noise reduction in CT by applying BF on CT image space is feasible.

References

[1] S. C. Bushong, "Radiologic Science for technologist: Physics, Biology, and Protection", 9th edition, Edited Rebecca Swisher, MOSBY Publishers, St. Louis Missouri USA, Chapter 23, **(2008)**, pp. 367-393.

[2] K. M. Hanson, "Noise and Contrast discrimination in computed tomography", Radiology of the Skull and Brain, Vol. 5: Technical Aspects of computed tomography. Edited Newton T H and Potts D G., C.V. MOSBY Publishers, St. Louis Missouri USA, Chapter 113, **(1981)**, pp. 3941-3955.

[3] P. Sprawls, "CT image detail and noise", Radiographics, vol. 12, **(1992)**, pp. 1041-1046.

[4] L. Yu, X. Liu, S. Leng, J. M. Kofler. J. C. Ramirez-Geraldo, M. Qu, J. Christner, J. G. Fletcher and C. H. McCollough, "Radiation dose reduction in computed tomography: techniques and future perspective", Imaging Med., vol. 1, no. 1, **(2009)**, pp. 65-84.

[5] N. Chun-yu, L. Shue-fen and Q. Ming, "Research on Removing Noise in Medical Image based on Median Filter method", IEEE International Symposium on IT in Medicine & Education, Jinan-China, **(2009)** August, pp. 384-388.

[6] Z. S. Kelm, D. Blezek, B. Bartholmai and B. J. Erickson, "Optimizing Non-Local Means for Denoising Low Dose CT", IEEE International Symposium on Biomedical Imaging: From Nano to Macro, Boston-USA, (2009) 28th June–1st July, pp. 662-665.

[7] A. M. L. Lanzolla, G. Andria, F. Attivissimo, G. Cavone, M. Spadavecchia and T. Magli, "Denoising Filter to Improve the Quality of CT images", IEEE Instrumentation and Measurement Technology Conference(I2MTC), 5-7 May, Singapore-Indonesia, **(2009)**, pp. 947–950.

[8] F. Attivissimo, G. Cavone, A. M. L. Lanzolla and M. Spadavecchia, "A Technique to Improve the Image Quality in Computer Tomography", IEEE Transaction on Instrumentation and Measurement, vol. 59, no. 5, **(2010)**, pp. 1251-1257.

[9] T. Li, X. Li, J. Wang, J. Wen, H. Lu, J. Hsieh and Z. Liang, "Nonlinear Sinogram Smoothing for Low-Dose X-Ray CT", IEEE Transaction on Nuclear Science, vol. 51, no. 5, **(2004)**, pp. 2505-2513.

[10] C. Tomasi and R. Manduchi, "Bilateral Filtering for Gray and Color Images", Proceedings of the IEEE International Conference on Computer Vision, Bombay-India, **(1998)** January 4-7, pp. 839-846.

[11] G. Vijaya and V. Vasudevan, "A Novel Noise Reduction Method using Double Bilateral Filtering", European Journal of Scientific Research, vol. 46, no. 3, **(2010)**, pp. 331-338.

[12] W. Q. Feng, S. M. Li and K. L. Zheng, "A Non-Local Bilateral Filter for Image Denoising", IEE International Conference on Apperceiving Computing and Intelligence Analysis (ICACIA), Chengdu-China, **(2010)** December 17-19, pp. 253 – 257.

[13] J. R. Giraldo, S. Leng, L. Yu and C. McCollough, "20-Fold dose reduction using a gradient adaptive bilateral filter: demonstration using in vivo animal perfusion CT", Medical Physics, vol. 37, no. 6, **(2010)**, pp. 3372.

[14] J. R. Giraldo, Z. S. Kelm, L. S. Guimaraes, L. Yu, J. G. Fletcher, B. J. Erickson and C. McCollough, "Comparative Study of Two Image Space Noise Reduction Methods for Computed Tomography: Bilateral Filter and Nonlocal Means", 31st Annual International Conference of the IEEE EMBS, Minneapolis-USA, **(2009)** September 2-6, pp. 3529-3532.

[15] S. Steckmann and M. Kachelrieß, "Blooming Artifact Reduction for Cardiac CT", Nuclear Science Symposium Conference Record (NSS/MIC) IEEE. Knoxville-USA, **(2010)** October 30 – November 6, pp. 2030–2035.
[16] J. Huang, L. Ma, N. Liu, Q. Feng and W. Chen, "Projection Data Restoration Guided Non-Local Means for Low-Dose Computed Tomography Reconstruction", IEEE International Symposium on Biomedical Imaging: From Nano to Macro, Chicago-UAS, **(2011)** 30th March - 2nd April, pp. 1167–1170.
[17] A. Manduca, L. Yu, J. M. Kofler, C. M. McCollough, J. G. Fletcher, J. D. Trzasko and N. Khaylova, "Projection space denoising with bilateral filtering and CT noise modeling for dose reduction in CT", Medical Physics, vol. 36, no. 11, **(2009)**, pp. 4911-4919.
[18] R. Gonzales and R. Woods, "Digital Image Processing", 3rdEdition. Edited Marcia J. Horton, PEARSON Prentice Hall Publishers, New Jersey USA, Chapter 11, **(2008)**, pp. 822-836.

Authors

Abdel-Razzak Al-Hinnawi

Earned a Ph.D in Digital Image Processing in 1999 from the University of Aberdeen in the United Kingdom, a MSc in Medical Imaging Systems from the same university, and a BSc in Bio-Medical Engineering from Damascus University in Syria. Since completion of his doctoral degree, he worked as Assistant Professor in the Biomedical Engineering Department of Damascus University in Syria between 1999 and 2005, and then he was promoted to be Associate Professor since 2005. During this period he was hosted to lecture at various universities. His main Research area is Medical Imaging and Image Processing topics.

Mohammed Daear

Earned a B.Sc. in Biomedical Engineering from Misr University for Science and Technology, Cairo, Egypt in 2009.

M.Sc. student in Medical Image Processing at Biomedical Engineering Department, Damascus University.